Molecular Crystals and Liquid Crystals

Publication details, including instructions for authors and subscription information:
http://www.tandfonline.com/loi/gmcl20

Raman Vibrational Properties of Carbon Nanotubes with the Radiation Defect Formation

O. P. Dmytrenko [a], N. P. Kulish [a], N. M. Belyi [a], S. V. Lizunova [a], Yu. I. Prylutskyy [a], L. Valkunas [b], R. Karpicz [b], V. V. Shlapatskaya [c], E. V. Prilutskiy [d], T. Wade [e] & J.-E. Wegrowe [e]

[a] Taras Shevchenko National University, Kyiv, Ukraine

[b] Institute of Physics, Laboratory of Molecular Compounds Physics, Vilnius, Lithuania

[c] Pisarzhevsky Institute of Physical Chemistry of NASU, Kyiv, Ukraine

[d] Institute for Problems of Materials Science of NASU, Kyiv, Ukraine

[e] Ecole Polytechnique, Laboratoire des solides irradiés, CNRS-UMR, Palaiseau Cedex, France

Version of record first published: 10 Jun 2010

To cite this article: O. P. Dmytrenko, N. P. Kulish, N. M. Belyi, S. V. Lizunova, Yu. I. Prylutskyy, L. Valkunas, R. Karpicz, V. V. Shlapatskaya, E. V. Prilutskiy, T. Wade & J.-E. Wegrowe (2008): Raman Vibrational Properties of Carbon Nanotubes with the Radiation Defect Formation, Molecular Crystals and Liquid Crystals, 497:1, 38/[370]-45/[377]

To link to this article: http://dx.doi.org/10.1080/15421400802458274

Mol. Cryst. Liq. Cryst., Vol. 497, pp. 38/[370]–45/[377], 2008

ISSN: 1542-1406 print/1563-5287 online
DOI: 10.1080/15421400802458274

Raman Vibrational Properties of Carbon Nanotubes with the Radiation Defect Formation

O. P. Dmytrenko[1], N. P. Kulish[1], N. M. Belyi[1], S. V. Lizunova[1], Yu. I. Prylutskyy[1], L. Valkunas[2], R. Karpicz[2], V. V. Shlapatskaya[3], E. V. Prilutskiy[4], T. Wade[5], and J.-E. Wegrowe[5]

[1]Taras Shevchenko National University, Kyiv, Ukraine
[2]Institute of Physics, Laboratory of Molecular Compounds Physics, Vilnius, Lithuania
[3]Pisarzhevsky Institute of Physical Chemistry of NASU, Kyiv, Ukraine
[4]Institute for Problems of Materials Science of NASU, Kyiv, Ukraine
[5]Ecole Polytechnique, Laboratoire des solides irradiés, CNRS-UMR, Palaiseau Cedex, France

Studies of changes in the crystal structure of multi-walled carbon nanotubes (MWNT) during the high-energy electron irradiation ($E_e = 1.8\,MeV$) *with doses from 3.0 to 10.0 MGy are carried out by means of the analysis of the Raman vibrational spectra. It is shown that defects generated by the electron beam irradiation are accompanied by an increase in the interlayer correlations as a consequence of interlayer links and local variations in the geometry of MWNT. The generation of the structural defects leads to the drop in the integral intensities of the G- and D-bands in the Raman scattering spectrum and to the splitting of the G-band into several components. These results are supported by the manifestation of new vibrational modes with increase in the fluence of irradiation which is an indication of the reconstruction of the structure and geometry of MWNT and, respectively, of their symmetry.*

Keywords: electron irradiation; multi-walled carbon nanotubes; Raman scattering

This work was partly supported by the joint Ukrainian-Lithuanian grant and the "Dnipro" Program. The authors are also thankful to Prof. V. Gulbinas and Dr. G. Niaura for valuable discussions.

Address correspondence to R. Karpicz, Institute of Physics, Laboratory of Molecular Compounds Physics, 231 Savanoriu Ave., Vilnius, LT-02300, Lithuania E-mail: renata@ar.fi.lt

INTRODUCTION

Most properties of nanoscale systems are radically different from those of their bulk analogues due to the space confinement. Moreover, by tuning the space restriction or by changing the concentration of atomic scale defects, the substantial variability of different physical characteristics can be achieved. Carbon nanotubes are typical examples of such systems demonstrating the variability of their properties as a result of the space confinement. A single-walled carbon nanotube (SWNT) can be considered as a roll-up of a two-dimensional (2D) graphene sheet. The diameter of a SWNT is typically of the order of nanometers with the aspect ratio exceeding 10^4, and its structure is uniquely described by a pair of indices (n, m) that define the diameter and chirality [1]. Depending on its structure, a SWNT can exhibit either metallic or semiconducting properties with structure-specific transition energies between quantized electronic states [1,2]. These unique electronic features in combination with other remarkable physical properties make SWNTs an ideal choice for a wide range of nanoscale applications such as nanometer-sized conducting wires, field effect transistors, and molecular electronics [3]. The electronic transition bands of semiconducting nanotubes can be attributed either to optical transitions between the van Hove singularities of the valence and conduction bands of (quasi)-1D systems defined according to the tight-binding approximation with a subsequent relaxation of charged carriers [1,4,5] or to excitonic transitions [6–10] with inclusion of multiparticle interactions, as follows from theoretical calculations [11,12]. A multi-walled carbon nanotube (MWNT) is composed of a set of concentrically arranged SWNTs of different radii. Due to van der Waals-type interactions between graphene sheets, the MWNT can be qualified in a similar way [13] with some additional impacts due to the intersheet interactions.

The Raman spectra of carbon nanotubes demonstrate many features that can be identified by specific phonon modes and can provide us with detailed information about their 1D feature and structural imperfections [14]. The strong and nonmonotonic dependence of the Raman spectra on the excitation wavelength displays the resonance transitions of the electron excitation between the van Hove singularities jointly with the absorption/emission of relevant phonons [14,15]. Because of small aspect ratio, the optical transitions exhibit the van Hove singularities with very large magnitudes giving rise to the enhancement in the Raman intensity. As a result, the resonance transitions are well distinguished from the individual SWNT spectra [16,17]. The so-called radial breathing mode (RBM), the graphene

band (G-band), the diffusion band (D-band), and the G′-band are the typical Raman-active phonon modes for nanotubes [16,17].

Transmission microscopy has shown that MWNTs of large diameter contain a considerable amount of defects. The presence of defects is also confirmed by variability of the fluorescence and Raman spectra of individual SWNTs [18,19]. As recently demonstrated by analyzing the Raman spectrum of the MWNT, the D-band and G-band are sensitive to the defects generated by electron beam irradiation [20]. These results were obtained by irradiating the polymer matrix containing the MWNTs with a high-energy electron beam ($E_e = 3.5\,\text{MeV}$) of different intensities. However, no systematic analysis of the spectral properties influenced by defects and/or lattice imperfections has been performed yet. Here, we demonstrate the sensitivity of the Raman spectra of MWNTs on the amount of defects generated by electrons of the energy $E_e = 1.8\,\text{MeV}$, which is high enough for the Frenkel pairs to be generated, as has recently been established [21–23]. The influence of the Frenkel pairs on the G-band, the D-band and the G′-band is considered.

MATERIALS AND METHODS

MWNTs were produced by means of the HiPCO (High-pressure catalytic decomposition of carbon monoxide) method with iron, cobalt, and nickel oxides used as catalysts. Predictability of the nanocarbon product formation is the advantage of this method. Parasitic carbon forms (soot, amorphous carbon, etc.), which are characteristic of the high-temperature processes of hydrocarbon conversion, are negligible in this case, since the pressure of the carbon vapour at the process temperature of $500 \pm 40^{\circ}\text{C}$ is small, and the formation of any noticeable particles by their homogeneous condensation is thermodynamically impossible.

Samples used for measurements of the Raman scattering spectra were prepared by means of compression at 5 bars as tablets of 2 mm in thickness.

For electron irradiation, the linear electron accelerator with doses from 3.0 to 10 MGy was used. Raman spectra were obtained with a monochromator (DFS-24) equipped with a 1200 lines/mm grating and FEU-62 and FEU-100 detectors. The integration time was 2 h. Each spectrum was recorded by accumulation of 3 scans. For the Raman scattering, the 514.5 nm-irradiation of an Ar+ laser (LGN-503) was used. The laser beam was focused on a spot of about 0.1 mm in diameter. The power density of the laser irradiation was always less than $5\,\text{W/cm}^2$. Measurements were performed at room

temperature. The X-ray diffractometry was used for visualization and for studies of the structural changes of MWNTs.

RESULTS AND DISCUSSION

The MWNTs of the length of hundreds of nanometers were obtained as shown in Figure 1. The strong resonance enhancement in the Raman spectra makes it possible to observe the Raman spectrum of nanotubes of a single type when the energy of the incident or scattered light is in resonance with the energy of a particular excitonic transition. The Raman spectra obtained by using the laser excitation at 514.5 nm are presented in Figure 2. Three characteristic bands of MWNTs are visible in the vicinity of 1353 cm^{-1} (D-band), 1589 cm^{-1} (G-band), and 2693 cm^{-1} (G′-band) (Fig. 2a) [24,25]. The D band is associated with the disorder-induced mode of graphene carbon, while the G-band is attributed to in-plane vibrations [24]. The G′-band is resulted from the two-photon scattering and characterizes the ordering of the graphene structure [24–26].

FIGURE 1 Visualization of a typical MWNT by means of TEM which was used for measurements.

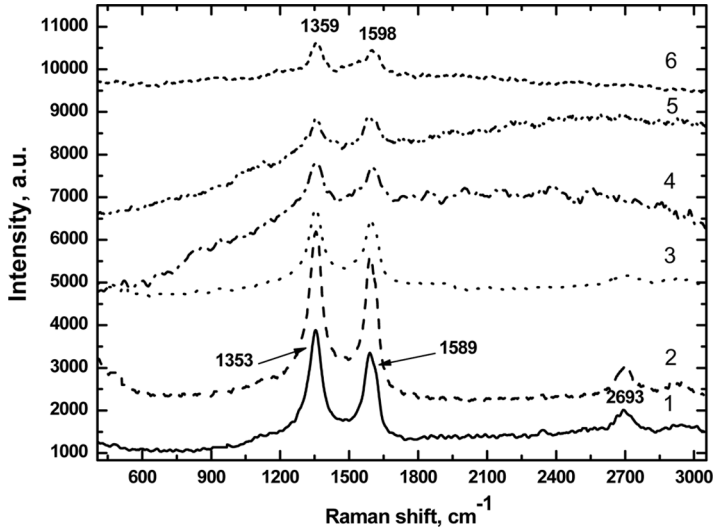

FIGURE 2 Raman scattering spectra of a MWNT in the initial (nonirradiated) state (1) and after the electron beam irradiation with doses of 3.0 (2), 4.0 (3), 6.0 (4), 80 (5), and 10.0 MGy (6); $\lambda_{ex} = 514.5\,\text{nm}, E_e = 1.8\,\text{MeV}$.

It is worth to note that all these resonance bands become weaker, as the dose of electron irradiation increases. This observation allows us to conclude that the amount of defects responsible for a distortion of the periodic structure of carbon nanotubes gradually increases with the dose of irradiation. Due to the complex composition of a Frenkel defect which contains both the interstitial atoms and vacancies in the carbon network, some changes in the interplanar spacing d_{002} are evidently expected. The changes in the lattice constant are also expected, as it follows from our recent X-ray diffraction data (not shown). From the shift of the diffraction maximum related to d_{002} to the larger angles, we can conclude that the lattice constant decreases with increase in the dose up to 4.0 MGy and slightly increases when the doses are in the range from 6.0 to 10.0 MGy.

In addition to the decrease in the intensity, all bands shift to higher energies (see Fig. 2). In contrast to the small doses of 0.5, 1.0, 1.5, and 2.0 MGy used in [27], where no band shape changes were observed, the Raman spectrum in our case essentially changes at large irradiation doses. The maxima of the D-, G-, and G′-bands in the samples prior to their irradiation are at 1353 cm^{-1}, 1589 cm^{-1}, and 2693 cm^{-1}, respectively, and shift to 1354 cm^{-1}, 1595 cm^{-1}, and 2698 cm^{-1} positions, when 4.0 MGy of irradiation has been applied. The shift of all bands

demonstrates some irregularity with a further increase of the irradiation. The maxima of the D- and G-bands are positioned at 1359 cm^{-1} and 1598 cm^{-1} at 10.0 MGy, respectively (see Fig. 3), while the G′-band is not visible anymore. A decrease in the G′-band intensity is consistent with a reduction in the degree of ordering of the graphene structures and the formation of carboneous side-products on irradiation [24].

In contrast to the results indicating the changes in the D-band observed for SWNTs and the graphene sheets as a result of irradiation with γ-quanta [28], the changes of the G-band caused by the ${}_0A_0^+$ and ${}_0E_2^+$ vibrational modes are also distinguished [29–31].

Decomposition of the D- and G-bands into the components is shown in Figure 3. Depending on the irradiation dose, the G-band clearly

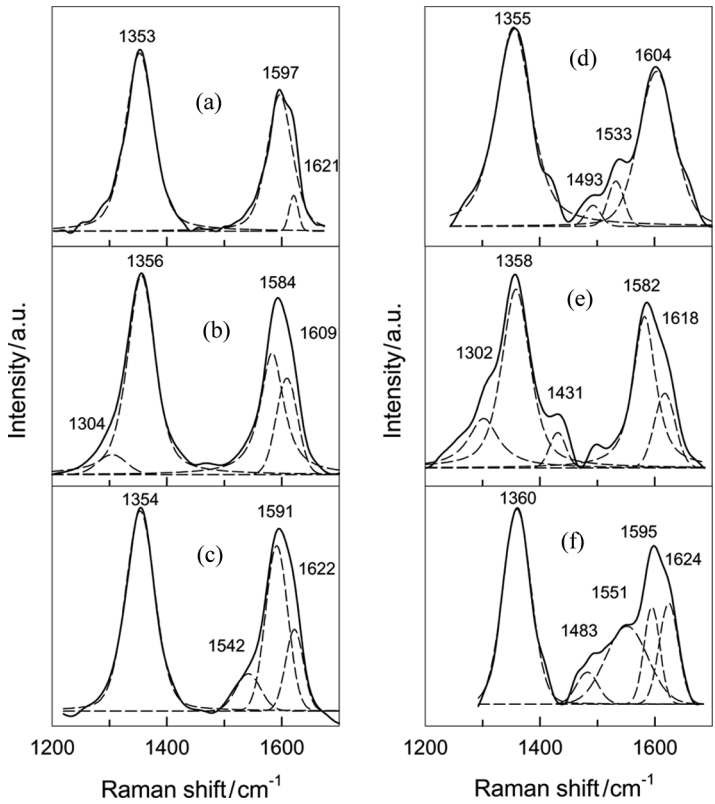

FIGURE 3 Decomposition of the Raman scattering spectra of the initial (nonirradiated) state of a MWNT (a) and those obtained after the electron beam irradiation with doses of 3.0 (b), 4.0 (c), 6.0 (d), 8.0 (e), and 10.0 MGy (f) in the vicinity of the G- and D-bands.

splits into several components. At a lower dose (Fig. 3b), two components are clearly visible in the vicinity of 1584 and 1609 cm^{-1}. The higher frequency component was attributed to the defective graphene mode, the D′-band [26]. The relative intensity of this mode with respect to that of the lower-frequency G-band component clearly increases for the highly irradiated sample (Fig. 3f), by indicating an increase in the disorder of the nanotube structure. It should be noted that an additional low-frequency component in the vicinity of 1542–1533 cm^{-1} appears at higher irradiation doses (Figs. 3c, d, and f). This feature broadens considerably (full width at half maximum, FWHM = 86 cm^{-1}) at the 10.0-MGy dose (Fig. 3f). Such spectral changes can be attributed to the charge transfer processes [25] as a result of the presence of defects.

Changes of the G-band shape due to a large dose of irradiation allow us to conclude about differences in the radiation damages, as was already assumed previously. If we proceed from the assumption about an increase in the interlayer ordering with increase in the dose of irradiation, then it is necessary to assume that the irradiation contributes to the structural variability in some parts of MWNTs and to a change in the type of the hybridization of electronic states with increase in the concentration of sp^3-bonds which are responsible for the formation of links of separate graphene layers.

It is worth to note that both effects obtained in our experiments, i.e., the obvious decrease in the intensities of the Raman bands and their shift to larger energies by increasing the irradiation doses (Fig. 2), were not obtained by using the electron beam of higher energies [20]. In that case, the D-band shifted to lower energies, while the position of the G-band was unchanged. Their intensities also did not decrease, and even some increase in their intensities with increase in irradiation doses was evident [20]. These differences in the changes of the Raman spectra induced by the electron beams with different electron energies could be considered as an indication that the defects generated by irradiation at different electron energies should be different in their origin. As follows from our results, the electron energies of 1.8 MeV are responsible for the generation of Frenkel defects, while defects of another type are generated when the twice greater electron energies (3.4 MeV) are used in the beam.

REFERENCES

[1] Saito, S., Dresselhaus, G., & Dresselhaus, M. S. (1998). *Physical Properties of Carbon Nanotubes*, Imperial College Press: London.
[2] Odom, T. W., Huang, J.-L., Kim, P., & Lieber, C. M. (2000). *J. Phys. Chem. B*, *104*, 2794.

[3] Baughman, R. H., Zakhidov, A. A., & de Heer, W. A. (2002). *Science*, *297*, 787.
[4] Lauret, J.-S., Voisin, C., Cassabois, G., Delalande, C., Roussignol, Ph., Jost, O., & Capes, L. (2003). *Phys. Rev. Lett*., *90*, 057404.
[5] Ostojic, G. N., Zaric, S., Kono, J., Strano, M. S., Moore, V. C., Hauge, R. H., & Smalley, R. E. (2004). *Phys. Rev. Lett*., *92*, 117402.
[6] Korovyanko, O. J., Sheng, C.-X., Vardeny, Z. V., Dalton, A. B., & Baughman, R. H. (2004). *Phys. Rev. Lett*., *92*, 017403.
[7] Ma, Y.-Z., Stenger, J., Zimmenrmann, J., Bachilo, S. M., Smalley, R. E., Weisman, R. B., & Fleming, G. R. (2004). *J. Chem. Phys*., *120*, 3368.
[8] Ma, Y.-Z., Valkunas, L., Dexheimer, S. L., Bachilo, S. M., & Fleming, G. R. (2005). *Phys. Rev. Lett*., *94*, 157402.
[9] Ma, Y.-Z., Valkunas, L., Bachilo, S. M., & Fleming, G. R. (2005). *J. Phys. Chem. B*, *109*, 15671.
[10] Wang, F., Dukovic, G., Brus, L. E., & Heinz, T. F. (2005). *Science*, *308*, 838.
[11] Spataru, C. D., Ismail-Beigi, S., Benedict, L. X., & Louie, S. G. (2004). *Phys. Rev. Lett*., *92*, 077402.
[12] Spataru, C. D., Ismail-Beigi, S., Benedict, L. X., & Louie, S. G. (2004). *Appl. Phys. A*, *78*, 1129.
[13] Hertel, T., Hagen, A., Talalaev, V., Arnold, K., Hennrich, F., Kappes, M., Rosenthal, S., McBride, J., Ulbricht, H., & Flahaut, E. (2005). *Nano Lett*., *5*, 511.
[14] Dresselhaus, M. S., Dresselhaus, G., Saito, R., & Jorio, A. (2005). *Phys. Rep*., *409*, 47.
[15] Dresselhaus, M. S., Dresselhaus, G., & Jorio, A. (2004). *Annu. Rev. Mater. Res*., *34*, 247.
[16] Jorio, A., Saito, R., Hafner, J. H., Lieber, C. M., & Hunter, M. (2001). *Phys. Rev. Lett*., *86*, 1118.
[17] Htoon, H., O'Connell, M. J., Doorn, S. K., & Klimov, V. I. (2005). *Phys. Rev. Lett*., *94*, 127403.
[18] Hartshuh, A., Pedrosa, H. N., Novotny, L., & Krauss, T. D. (2003). *Science*, *301*, 1354.
[19] Htoon, H., O'Connell, M. J., Cox, J. P., Doorn, S. K., & Klimov, V. I. (2004). *Phys. Rev. Lett*., *93*, 027401.
[20] Sullivan, M. E., Klosterman, D., & Palmese, G. R. (2007). *NIM B*, *265*, 352.
[21] Zaiser, M. & Banhart, F. (1997). *Phys. Rev. Lett*., *79*, 3680.
[22] Zaiser, M., Lyutovich, Y., & Banhart, F. (2000). *Phys. Rev. B*, *62*, 3058.
[23] Banhart, F. (2002). *Sol. St. Phys*., *44*, 388.
[24] DiLeo, R. A., Landi, B. J., & Raffaelle, R. P. (2007). *J. Appl. Phys*., *101*, 064307.
[25] Mattia, D., Rossi, M. P., Kim, B. M., Korneva, G., Bau, H. H., & Gogotsi, Y. (2006). *J. Phys. Chem. B*, *110*, 9850.
[26] Jorio, A., Pimenta, M. A., Souza Filho, A. G., Saito, R., Dresselhaus, G., & Dresselhaus, M. S. (2003). *New J. Phys*., *5*, 139.1.
[27] Ritter, U., Scharff, P., Siegmund, C., Dmytrenko, O. P., Kulish, N. P., Prylutskyy, Yu. I., Belyi, N. M., Gubanov, V. A., Komarova, L. A., Lizunova, S. V., Poroshin, V. G., Shlapatskaya, V. V., & Bernas, H. (2006). *Carbon*, *44*, 2694.
[28] Hulman, M., Skakalova, V., Roth, S., & Kuzmany, H. (2005). *J. Appl. Phys*., *98*, 024311.
[29] Terrones, M., Souza Filho, A. G., & Rao, A. M. (2008). Doped carbon nanotubes: Synthesis, characterization and applications. In: *Carbon Nanotubes*, Jorio, A., Dresselhuas, G., & Dresselhaus, M. (Eds.), Springer: Berlin, p. 531–566.
[30] Damnjanović, M., Milošević, I., Vukolić, T., & Stedanović, R. (1999). *Phys. Rev. B*, *60*, 2728.
[31] Dobardžić, E., Milošević, I., Nikolić, B., Vukolić, T., & Damnjanović, M. (2003). *Phys. Rev. B*, *68*, 045408.